Published in final edited form as:
Proc SPIE. 2012 January 21; 8228: . doi:10.1117/12.909470.

Parallel multispot smFRET analysis using an 8-pixel SPAD array

A. Ingargiola[a,b,*], **R. A. Colyer**[b], **D. Kim**[c], **F. Panzeri**[a], **R. Lin**[b], **A. Gulinatti**[a], **I. Rech**[a], **M. Ghioni**[a], **S. Weiss**[b], and **X. Michalet**[b,*]

[a]Dipartimento Elettronica ed Informazione, Politecnico di Milano, Milan, Italy

[b]Department of Chemistry & Biochemistry, UCLA, Los Angeles, CA USA

[c]Nesher Technologies Inc, Los Angeles, CA USA

Abstract

Single-molecule Förster resonance energy transfer (smFRET) is a powerful tool for extracting distance information between two fluorophores (a donor and acceptor dye) on a nanometer scale. This method is commonly used to monitor binding interactions or intra- and intermolecular conformations in biomolecules freely diffusing through a focal volume or immobilized on a surface. The diffusing geometry has the advantage to not interfere with the molecules and to give access to fast time scales. However, separating photon bursts from individual molecules requires low sample concentrations. This results in long acquisition time (several minutes to an hour) to obtain sufficient statistics. It also prevents studying dynamic phenomena happening on time scales larger than the burst duration and smaller than the acquisition time. Parallelization of acquisition overcomes this limit by increasing the acquisition rate using the same low concentrations required for individual molecule burst identification. In this work we present a new two-color smFRET approach using multispot excitation and detection. The donor excitation pattern is composed of 4 spots arranged in a linear pattern. The fluorescent emission of donor and acceptor dyes is then collected and refocused on two separate areas of a custom 8-pixel SPAD array. We report smFRET measurements performed on various DNA samples synthesized with various distances between the donor and acceptor fluorophores. We demonstrate that our approach provides identical FRET efficiency values to a conventional single-spot acquisition approach, but with a reduced acquisition time. Our work thus opens the way to high-throughput smFRET analysis on freely diffusing molecules.

Keywords

single-molecule; photon counting; FRET; SPAD array; high throughput

1. INTRODUCTION

In recent years single-molecule Förster resonance energy transfer (smFRET) has gained widespread acceptance in biology as an effective technique to monitor distances between two or more fluorophores[1–4]. The single-molecule approach allowed to investigate interactions of proteins with nucleic acids or conformational changes of macromolecules with an accuracy impossible to achieve with ensemble measurements[5–8]. smFRET measurements are performed either on surface-immobilized or on freely diffusing molecules. The latter approach has the advantage to be immune to surface interactions which may influence the observed dynamics.

[*]ingargiola.antonino@gmail.com, michalet@chem.ucla.edu; phone 1-310-794-6693.

In freely diffusing smFRET measurements a single-molecule generates a photon burst while diffusing through a small excitation volume (~1fL). The low sample concentration (<100pM) needed to have at most one molecule a time in the excitation volume, requires long acquisition times (tens of minutes to one hour) in order to collect a number of bursts sufficient for FRET analysis. This results not only in time-consuming measurements but, more importantly, makes very difficult to study dynamic phenomena on timescales of a minute or less.

A high-throughput FRET approach can overcome these limitations enabling the observation of faster dynamics at the single-molecule level. In order to achieve this goal, the sample needs to be excited by several spots simultaneously, and photons emitted in each excitation volume must be detected and processed in parallel. The multispot approach poses several challenges both in the generation of the excitation spots and in the detection system. The excitation pattern can be obtained either making use of micro-lenses or employing a spatial light modulator. For the detection part, employing single-pixel *Single-Photon Avalanche Diodes* (SPAD's) as in traditional smFRET system is not possible, due to the overwhelming complexity and cost involved in managing and aligning a large number of detectors. Recent advances in detector technology led to the development of SPAD arrays suitable for single-molecule spectroscopy[9]. Multispot excitation has been reported for *fluorescence correlation spectroscopy* (FCS) measurements employing small arrays of SPAD's [10,11]. No report of multispot smFRET measurements exists to date.

In this work we report the first multispot smFRET system, which features 4 excitation spots and parallel detection of the fluorescence signal of each spot on two color channels. We employed a *liquid crystal on silicon* (LCOS) spatial light modulator for the generation of excitation spots and a custom 8×1 SPAD array (SPADA) as the detector. The system has been employed to measure a set of double-stranded DNA (dsDNA) samples, labeled by dyes attached at different distances. This gave a spectrum of FRET efficiency values suitable to assess the performances of the system.

2. INSTRUMENTS AND METHODS

2.1 Setup description

A schematic representation of the setup is reported in Figure 1, which is very similar to the arrangement described previously[10]. Briefly, the sample is excited by 4 linearly arranged diffraction-limited spots focused into the sample using a high numerical aperture (NA) water-immersion objective lens (Olympus 60x, NA = 1.2). The fluorescence signal collected from these spots is split into two spectrally separated images for the donor and the acceptor components. Each component, comprised of 4 emission spots, is then focused onto one half of the 8×1 SPADA.

The 4-spot excitation pattern is generated using a collimated 532 nm laser beam (IC-532-1000 ps, High Q Laser) and a LCOS spatial light modulator (LCOS-SLM, or simply LCOS, model LCOS-SLM X1048, Hamamatsu) as previously described [10]. The modulation pattern on the LCOS is software-controlled, providing complete flexibility to specify the excitation pattern geometry (number of spots, pitch, position and orientation). This programmability is essential to facilitate a precise alignment of the setup, as described below.

The 4-spot emission pattern is recollimated by the objective lens and sent to the camera port of the microscope. A dual-view system (OptoSplit II Image Splitter, CAIRN Research Ltd.) allows focusing and aligning the spots on the detector, projecting the donor and acceptor spectral components on two halves of the SPAD array.

The detector is a monolithic 8×1 array of silicon SPAD's developed at the Politecnico di Milano employing a custom planar technology[9]. Each SPAD (or pixel) has a 50 μm diameter active area and is separated from its neighbor by 250 μm. The module outputs 8 independent streams of 50 ns wide TTL pulses corresponding to detected photons or dark counts from each SPAD pixel.

The 8 TTL SPADA outputs are fed to 8 inputs of a reconfigurable digital input/output board (PXI-7813R, National Instruments). This board features a Virtex-II 3M field-programmable gate array (FPGA), which can be used to time-tag each pulse with 12.5 ns precision, label it with the source SPAD pixel number and transfer the data to the host PC via a PXI-PCI communication bridge (PXI-PCI 8330, NI). The host PC is used to display, save and analyze the data. The FPGA is programmed using LabVIEW-FPGA and data acquisition and analysis on the PC are written in LabVIEW.

2.2 Alignment procedure

After separation into the donor and acceptor components, the 4 emission spots need to be reimaged onto the 8 equally spaced pixels of the SPAD detector. Spectral separation and imaging are performed by the dual-view system, which allows aligning the donor and acceptor images next to each other on the detector using alignment micrometer screws.

The pitch, position and orientation of the excitation spots can be modified using the software controlling the LCOS pattern. Changing any of these parameters affects both donor and acceptor images identically. In particular, changing the orientation of the pattern results into two (4-spot) images rotated around their own, distinct rotation center. To obtain two images which are aligned with one another in order to match the geometry of the detector, LCOS-independent degrees of freedom are necessary. These are provided by the dual-view manual controls, which allow repositioning each image (X and Y translation) with respect to the detector. Accurate alignment of the donor and acceptor images on the detector is of paramount importance to obtain the maximum collecting efficiency and the most even response between the donor and the acceptor channels.

Alignment is performed in two steps: the first step is performed only once during initial setup assembly, while the second, fine alignment step, is performed before each measurement session.

During the first, coarse alignment step, the dichroic filter in the dual-view is replaced by a 50% beam splitter. This allows using a sample containing a single fluorophore in order to obtain identical signals in the donor and acceptor channels. First, we determine the optimal excitation spot pitch in order to match the pitch of the SPAD array. This is accomplished by placing a CCD camera at the exit port of the dual-view system and imaging a concentrated sample of Rhodamine 6G (R6G, ~3μM, Sigma Aldrich) illuminated with the LCOS-generated spot pattern. Knowing the pixel size of the camera, it is possible to directly measure the spot pitch in the image plane. Once the optimal pitch has been defined, the CCD camera is replaced by the SPAD array. A first coarse alignment is performed by positioning the SPAD detector in order to maximize the counts on all 8 channels. After this step, the detector position is locked in place on the dual-view exit port and the dichroic mirror is installed back into the dual-view system.

The second alignment step uses a concentrated (~1M) solution of Alexa 546 (Life Technologies), which can be excited with the 532 nm laser and whose emission can be detected in both the donor and acceptor channels. Its goal is to precisely determine the exact location, in the sample, of the optical conjugate of each SPAD pixel. For this purpose, we excite the sample with a single spot, which is translated in both X and Y directions using the

programmable LCOS, until the signal on one SPAD pixel is maximized. This allows determining the best conjugate location for that SPAD pixel on the LCOS. The procedure is then automatically repeated for each SPAD pixel, until a series of 8 ideal locations for all SPAD's has been determined. First, this allows fine-tuning the spot pitch, by direct measurement of the distance between the programmed spots. Finally, since only 4 points are excited in the sample (each one generating a signal on the donor and acceptor side of the detector), this allows detecting some residual orientation difference or offset between the SPAD array and the spot images. We then slightly adjust the spot image location using the dual-view controls and reiterate the procedure until a sufficiently good alignment is obtained. Using this approach, it is possible to achieve an alignment accuracy of both donor and acceptor channels of better than 7 μm. This is sufficient to center each ~ 30 μm diameter spot image onto its corresponding 50 μm diameter SPAD pixel.

Once the fine alignment step is completed, measurement of the single-molecule samples can proceed.

2.3 Data acquisition

The 8 TTL SPAD outputs are acquired by the acquisition board containing a Virtex II FPGA through a BNC connector breakout box (CA-1000, National Instruments). We programmed the FPGA to perform basic time-stamping of the incoming TTL pulses (12.5 ns resolution) and continuously (and asynchronously) send the pulses arrival times and channel numbers to the PC via direct memory access (DMA) first-in first-out (FIFO) transfer. The implementation uses 8 FIFO buffers on the FPGA to save the pulses arrival times. Cyclically, each local FIFO is queried and, if some data is available, a single pulse information is moved into a DMA communication FIFO. Data is binned on the host PC in real time using a user-defined resolution and displayed as a color-coded chart or time traces for each channels. In this configuration, burst search and FRET histogram analysis are performed off-line on the host computer.

We also tested a second approach in which the FPGA board performs not only time-tagging of the incoming pulses but also burst identification and data reduction. This hardware-based burst search significantly reduces the amount of data transferred to the PC and will be described elsewhere. Note that, in order to represent the live time traces, raw time stamps or binned time traces still need to be transferred from the FPGA.

2.4 Burst search algorithm

The burst search is performed on a single-spot basis (one donor and one acceptor channel) using a classical thresholding algorithm[12–14] applied on the merged streams of the donor and acceptor channels. Merging helps in detecting bursts, which have either a low donor or low acceptor count, which would be hard to detect individually. After burst detection, the respective number of donor and acceptor photons in each burst (donor and acceptor burst sizes), the burst duration, as well as start and stop times in each channel can be easily recovered.

The algorithm is efficiently implemented without binning the photon arrival times (saving memory and processing power). Instead, the photon stream is analyzed using a sliding window of duration T. When a window contains more than m photons, a burst is started; conversely, when the number of photons drops below m the burst ends. In other terms, m/T is the threshold rate above which a burst starts and below which a burst ends. Finally, only bursts with more than L photons are saved. Typical values for the burst search parameters are T = 0.5–1 ms, m = 3–10 and L = 20–50.

However, choosing a fixed set of burst search parameters is not optimal, particularly in a multi-pixel setup. In fact the background rate is different from pixel to pixel due to differences in the point spread function (PSF) of each excitation spot and differences in dark-counting rate (DCR) for each SPAD pixel. Additionally, background variations can be occasionally observed at the single spot level (due for instance to sample evaporation, drift or bleaching), which ideally require an adaptive threshold. In order to adaptively define optimal burst search parameters, the background rate must be computed on a spot-by-spot basis. Ideally we would choose a low threshold in order to detect bursts with maximum accuracy. In reality, the threshold rate can not be set too low, otherwise we risk to identify random background fluctuations as bursts. Practically, a threshold rate 2 or 3 times above the background rate is a good trade-off between rejecting noise and efficient burst detection. In the data presented in the next section, we computed the background rate before burst search for each SPAD pixel, set the threshold rate to 2.5 times the background rate (B), fixed $m = 3$ and calculated $T = m/(2.5\,B)$.

Once the bursts are identified, a proximity ratio (or raw FRET efficiency) can be computed for each burst:

$$E_{raw\,i} = \frac{F_{ai}}{F_{ai} + F_{di}}, \qquad i = 1, 2, 3, 4 \quad (1)$$

where F_{ai} is the number of photons in the acceptor channel and F_{di} the number of photon in the donor channel, and the index i denotes one of the 4 excitation spots. This *proximity ratio*[13] needs to be corrected for background and leakage of the donor emission in the acceptor channel[15]. For background compensation new corrected burst sizes can be compute according to:

$$F'_{ai} = F_{ai} - W_{ai} \cdot B_{ai} \quad (2)$$

$$F'_{di} = F_{di} - W_{di} \cdot B_{di} \quad (3)$$

In eq. (2) and (3), W_{ai} and W_{di} are the burst durations in the acceptor (*ai*) and donor (*di*) channel, and B_{ai} and B_{di} are the background rates for the acceptor and donor channel. As before, i indicates the excitation spot.

Leakage is due to the broad band emission of the donor fluorophore, which usually has a tail extending in the acceptor emission wavelength range. For a given set of filters and fluorophore, the leakage can be precisely determined experimentally by using a donor only sample and measuring the observed signal in the acceptor channel. Leakage is expressed as a percentage of the donor channel signal. Calling k_{da} the leakage percentage, we can correct the acceptor burst sizes as follows:

$$F''_{ai} = F'_{ai} - k_{da} \cdot F'_{di} \quad (4)$$

Finally, in order to obtain the correct FRET efficiency, the different efficiency between the donor and the acceptor channel must be considered. This requires knowing the fluorophore quantum yield, emission spectrum, the optical transmittance of the entire optical system, and the photon-detection efficiency (PDE) of the detectors[3]. All these parameters are commonly included in a factor γ (see eq. (5)), that has to be determined experimentally for each pair of SPAD pixels.

$$E_i = \frac{F_{ai}}{F_{ai} + \gamma_i \cdot F_{di}} \quad (5)$$

Lee et al.[15] demonstrate a method for facile γ calculation which however requires employing an alternating laser excitation (ALEX). The ALEX technique requires employing a second laser for acceptor dye excitation and has not been implemented at this stage on the multispot smFRET setup. All values reported in the following are background- and leakage-corrected FRET values computed assuming $\gamma = 1$.

3. RESULTS

To test our smFRET setup we measured data from a set of double-stranded DNA (dsDNA) samples of various lengths (25 to 32 base pairs, bp), doubly-labeled with Cy3B (donor, Amersham) and ATTO 647N (acceptor, Atto-Tec Gmbh) fluorophores. The fluorophores were attached on complementary single-stranded DNA (ssDNA) molecules in order to obtain distances of 3, 5, 7, 9 bp. The samples were prepared by hybridization of the complementary labeled ssDNA oligonucleotides using standard procedures.

Figure 2 reports acceptor versus donor burst size scatter plots for the 5 bp sample. Two populations one of donor-only molecules (green dots) and one of FRET molecules (red dots) are noticeable. The selection of the two populations has been performed setting a threshold on the FRET value corresponding to the minimum between the two peaks in the FRET histogram. In Figure 2 the donor-only bursts lie along the horizontal axis. In those bursts, the acceptor counts are due mostly to background and there is no correlation between the acceptor and the donor burst sizes. Note that each burst size is corrected by subtracting a background value obtained according to eq. (2)–(3). The background noise variance results in a residual vertical spread for the donor-only bursts around the 0 value.[13]

Figure 3 shows the FRET histograms for the four different dsDNA samples. Each plot is comprised of 4 subplots, corresponding to the different pairs of SPAD pixels (or excitation spots). For all the measured samples, we obtained similar FRET histograms for each of the four spots. The FRET population (right histogram peak) is clearly distinguishable and an estimation of the FRET efficiency (FRET peak position, *E*) is possible and reported below each plot. We confirmed the correctness of these values using a standard single-spot ALEX-FRET setup. As expected, the position of the FRET population peak decreases with increasing distance between fluorophores. As noted in Figure 2, a significant zero-FRET population is present due to singly-labeled molecules. As experienced before the introduction of the ALEX approach, the presence of this subpopulation makes it difficult to measure low FRET values. This problem is inherent to all smFRET system employing a single excitation laser and can only be overcome by adding a second excitation laser to be able to identify the presence of an acceptor dye[15].

4. CONCLUSIONS AND PROSPECTS

We have reported the first multispot smFRET system, operating on freely diffusing molecules. The system works in parallel on 4 excitation spots, employing the 8 SPAD pixels of a monolithic custom SPAD array. We demonstrated the ability to discriminate FRET efficiencies corresponding to distances between Cy3B and ATTO 647N dyes which differ by 2 base pairs (0.6 nm). This resolution is comparable with the resolution of current state-of-the-art smFRET systems[2,3,16]. The multispot approach, however, allows a reduction of the acquisition time by a factor proportional to the number of SPAD pixels, making it possible to observe faster dynamics.

Several obvious improvements to the system are possible. First, the employed custom thin SPAD array has a photon-detection efficiency (PDE) typical for silicon planar SPAD (< 50%, reached at 550 nm). While the PDE is slightly higher than standard CMOS SPAD's, is not as high as the PDE of dedicated (non-planar) single-pixel SPAD's, which are however manufactured with a technology not compatible for integration in arrays[9,17]. A new red-enhanced process[18] has been recently developed at Politecnico di Milano, which is compatible with the fabrication of SPAD arrays. The availability of such red-enhanced detectors with a larger number of SPAD's would greatly enhance the performances of the system.

The next logical step consists in including an alternating laser excitation (ALEX) scheme[15] into the multispot approach in order to obtain better identification of singly- and doubly-labeled molecules. Such a system would enable very interesting new perspectives for high-throughput smFRET spectroscopy.

Lastly, the combination of an automated microfluidics sample handling system[19] with a multispot ALEX based system will greatly enhance solution-based smFRET experiment yielding high speed, high throughput and high content molecular analysis.

Acknowledgments

This work was supported by NIH grant R01 GM084327 and by NIH grant GM069709.

References

1. Weiss S. Fluorescence Spectroscopy of Single Biomolecules. Science. 1999; 283(5408):1676–1683. [PubMed: 10073925]
2. Weiss S. Measuring conformational dynamics of biomolecules by single molecule fluorescence spectroscopy. Nature Structural Biology. 2000; 7(9):724–9.
3. Michalet X, Weiss S, Jäger M. Single-molecule fluorescence studies of protein folding and conformational dynamics. Chemical Reviews. 2006; 106(5):1785–813. [PubMed: 16683755]
4. Bustamante C, Cheng W, Mejia YX. Revisiting the central dogma one molecule at a time. Cell. 2011; 144(4):480–97. [PubMed: 21335233]
5. Kapanidis AN, Margeat E, Laurence TA, Doose S, Ho SO, Mukhopadhyay J, Kortkhonjia E, Mekler V, Ebright RH, et al. Retention of transcription initiation factor sigma70 in transcription elongation: single-molecule analysis. Molecular Cell. 2005; 20(3):347–56. [PubMed: 16285917]
6. Kapanidis AN, Margeat E, Ho SO, Kortkhonjia E, Weiss S, Ebright RH. Initial transcription by RNA polymerase proceeds through a DNA-scrunching mechanism. Science. 2006; 314(5802): 1144–7. [PubMed: 17110578]
7. Wu JY, Stone MD, Zhuang X. A single-molecule assay for telomerase structure-function analysis. Nucleic Acids Research. 2010; 38(3):e16. [PubMed: 19920121]
8. Liu S, Abbondanzieri EA, Rausch JW, Le Grice SFJ, Zhuang X. Slide into action: dynamic shuttling of HIV reverse transcriptase on nucleic acid substrates. Science. 2008; 322(5904):1092–7. [PubMed: 19008444]
9. Rech I, Marangoni S, Resnati D, Ghioni M, Cova S. Multipixel single-photon avalanche diode array for parallel photon counting applications. Journal of Modern Optics. 2009; 56(2–3):326–333.
10. Colyer RA, Scalia G, Rech I, Gulinatti A, Ghioni M, Cova S, Weiss S, Michalet X. High-throughput FCS using an LCOS spatial light modulator and an 8 × 1 SPAD array. Biomedical Optics Express. 2010; 1(5):1408–1431. [PubMed: 21258559]
11. Gösch M, Serov A, Anhut T, Lasser T, Rochas A, Besse P-A, Popovic RS, Blom H, Rigler R. Parallel single molecule detection with a fully integrated single-photon 2×2 CMOS detector array. Journal of Biomedical Optics. 2004; 9(5):913–21. [PubMed: 15447011]

12. Eggeling C, Berger S, Brand L, Fries JR, Schaffer J, Volkmer A, Seidel Ca. Data registration and selective single-molecule analysis using multi-parameter fluorescence detection. Journal of Biotechnology. 2001; 86(3):163–80. [PubMed: 11257530]

13. Nir E, Michalet X, Hamadani KM, Laurence TA, Neuhauser D, Kovchegov Y, Weiss S. Shot-noise limited single-molecule FRET histograms: comparison between theory and experiments. The Journal of Physical Chemistry B. 2006; 110(44):22103–24. [PubMed: 17078646]

14. Selvin, PR.; Ha, T. Single-Molecule Techniques: A Laboratory Manual. Selvin, PR., editor. Vol. 507. Cold Spring Harbor Laboratory Press; 2008.

15. Lee NK, Kapanidis AN, Wang Y, Michalet X, Mukhopadhyay J, Ebright RH, Weiss S. Accurate FRET measurements within single diffusing biomolecules using alternating-laser excitation. Biophysical Journal. 2005; 88(4):2939–53. [PubMed: 15653725]

16. Dahan M, Deniz AA, Ha T, Chemla DS, Schultz PG, Weiss S. Ratiometric measurement and identification of single diffusing molecules. Chemical Physics. 1999; 247(1):85–106.

17. Cova S, Ghioni M, Lotito a, Rech I, Zappa F. Evolution and prospects for single-photon avalanche diodes and quenching circuits. Journal of Modern Optics. 2004; 51(9–10):1267–1288.

18. Gulinatti A, Panzeri F, Rech I, Maccagnani P, Ghioni M, Cova S. Planar silicon SPADs with improved photon detection efficiency. Proc of SPIE. 2011; 7945:79452P–10.

19. Hansen CL, Sommer MOa, Quake SR. Systematic investigation of protein phase behavior with a microfluidic formulator. Proceedings of the National Academy of Sciences of the United States of America. 2004; 101(40):14431–6. [PubMed: 15452343]

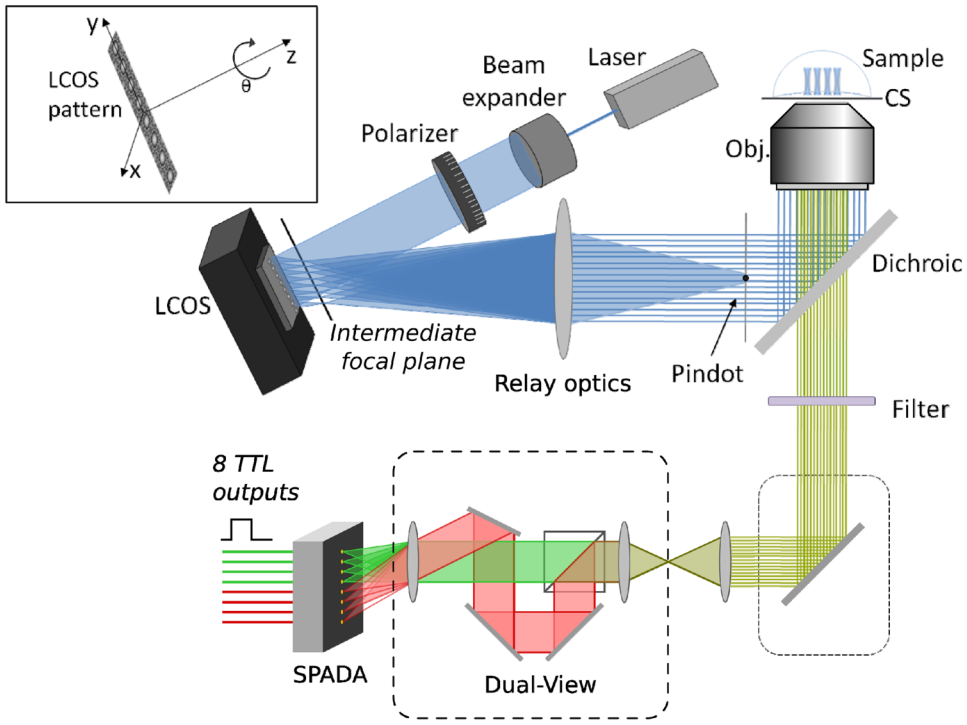

Figure 1.

Schematic representation of the multispot smFRET setup. A linear pattern of 4 excitation spots is generated at an intermediate focal plane using the LCOS. The excitation pattern is projected into the sample via the objective lens (Obj.) through a coverslip (CS). The resulting sample fluorescence is fed into the dual-view input and split into two separate images for the donor and acceptor spectral components. The SPADA acquires the 8 emission spot signals (4 for donor and 4 for acceptor) and provides 8 TTL outputs to the downstream acquisition board.

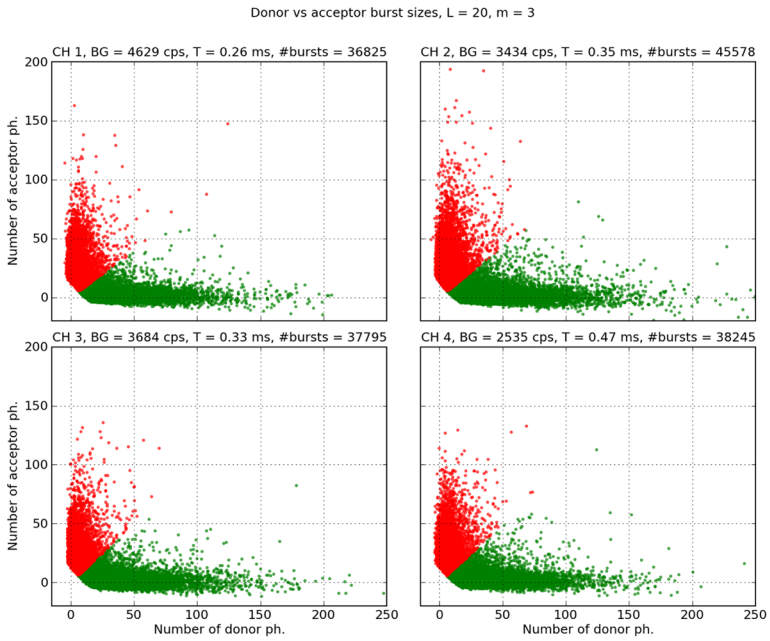

Figure 2.

Burst sizes of a dsDNA sample labeled with donor and acceptor dyes 5 base pairs apart. Scatter plots report the acceptor burst sizes versus the corresponding donor burst sizes for the 4 measurement spots. For each spot, the burst population is split in donor-only bursts (*green dots*) and in the "high FRET" population (*red dots*). The data is corrected for background and leakage of donor emission in the acceptor channel.

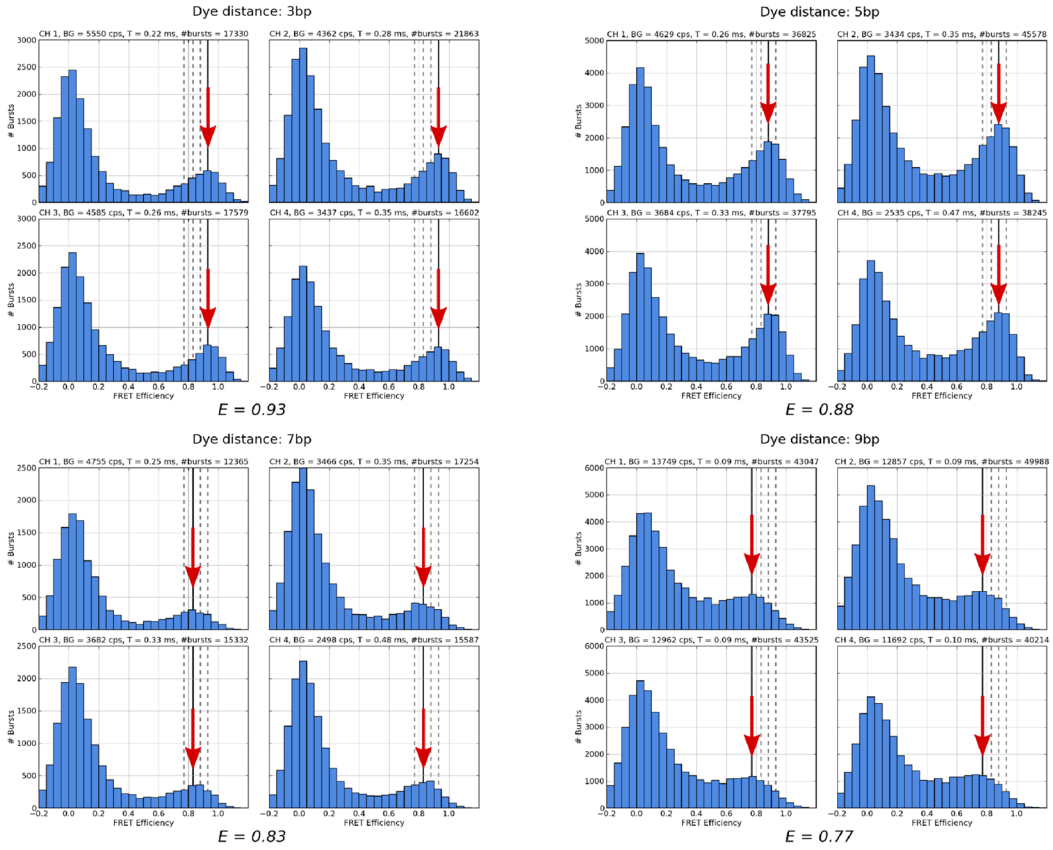

Figure 3.
FRET histograms for the dsDNA samples with distances between dyes of 3, 5, 7 and 9 base pairs. Within each sample quadrant, each histogram refers to a different excitation spot. The red arrows indicate the position (*E*) of the peak corresponding to the FRET population. For comparison, on each plot, the FRET efficiency of the other samples is reported as vertical dashed lines.